

NASA TECHNICAL
MEMORANDUM

NASA TM X- 62,304

NASA TM X- 62,304

(NASA-TM-X-62304) THEORETICAL STUDY OF
LIFT GENERATED VORTEX SHEETS DESIGNED TO
AVOID ROLL UP (NASA) 39 p HC \$4.00

N73-32976

CSCL 01A

G3/02

Unclas
19820

THEORETICAL STUDY OF LIFT-GENERATED VORTEX SHEETS
DESIGNED TO AVOID ROLL UP

Vernon J. Rossow

Ames Research Center
Moffett Field, Ca. 94035

September 1973

Theoretical Study of Lift-Generated Vortex Sheets

Designed to Avoid Roll Up

VERNON J. ROSSOW*

Ames Research Center, NASA, Moffett Field, California

ABSTRACT

The work described in this paper is based on the premise that lift-generated vortex sheets do not necessarily need to roll up. In order to explore this possibility, two vortex arrays are first designed, which do not roll up since it is specified that they rotate or translate as a unit due to their self-induced velocity field. These hypothetical arrays are then used to represent the vortex sheets shed by lifting wings. When the span loadings and the inviscid vortex wakes associated with these arrays are studied theoretically, the postulated motions are found to be unstable to disturbances; that is, the vortex elements behind a wing that sheds rotating arrays roll up into several vortices per side, while the wake behind a wing that sheds a translating array takes on a random or chaotic character. It is then indicated how these concepts could be applied to current large aircraft possibly to reduce the wake-vortex hazard.

Introduction

The vortices that trail behind lifting surfaces such as wings and helicopter rotor blades present undesirable and sometimes hazardous flow distortions to the lifting surfaces of aircraft entering that airspace. One solution is simply to avoid the regions occupied by these vortices.

* Staff Scientist. Associate Fellow AIAA.

Alternatively, since it may not always be possible to locate and avoid vortices, it becomes necessary to change the wake of the vortex generating aircraft, or the roll performance of the encountering aircraft, or both, so that acceptably safe flight can be sustained whether or not vortices are encountered. The substantial increase in roll control required by current small aircraft to fly safely into a vortex of a large aircraft forces consideration of methods for making vortices less hazardous. Past attempts to alleviate the vortex hazard include such methods as increased vortex diffusion by introducing turbulence into the vortex with generators (such as a wingtip spoiler)¹ by acceleration of an instability,² or by shaping the wing to generate a vortex that has a less intense core.³ A decrease in the lifetime or intensity of the vortices would presumably reduce the hazardous distance behind the generating aircraft. An acceptable solution is achieved when the hazardous distance behind the generating aircraft is commensurate with the distance based on other safety considerations used during landing and takeoff. Naturally, any acceptable vortex alleviation scheme must also satisfy a number of practical constraints before the solution is usable. A fairly complete discussion and summary of the considerable literature on the structure of lift-generated vortices, the possibilities for their modification, and the effect that a vortex might have on the motion of an encountering aircraft are given in a recent article by El-Ramly.⁴ Papers that relate to the present study are those^{3,5-10} that investigate theoretically or experimentally the effect of special wing planform shapes or span loading on the vortex structure.

Unlike past efforts, this work is based on the premise that vortex sheets do not necessarily need to roll up. That is, the rollup of vortex sheets illustrated in Fig. 1 which usually occurs is assumed to be suppressed here

◁ Fig. 1

by proper design of the span loading on the wing so that a fully-developed vortex structure does not occur. This concept was developed from the study described in Ref. 11 wherein an attempt was made to derive criteria that would indicate the centers of rollup for vortex sheets produced behind current large aircraft. In the course of that attempt, it occurred to the author that it might be possible to design vortex sheets that do not roll up, or at least not into the tightly bound, well organized vortex pairs typical of span loadings that are approximately elliptical. This paper first presents the design and theoretical study of two vortex sheets that should not roll up and then discusses the way in which these conceptual span loadings might be used to alleviate the aircraft wake vortex hazard of large aircraft.

Design of Vortex Sheets that do not Roll Up

The design of vortex sheets that should not roll up is accomplished by specifying that the self-induced motion on every element of the sheet does not change with time. In order to simplify the design problem, the vortex sheet is approximated in the so-called Trefftz plane (see Fig. 1) by a flat, two-dimensional vortex array. Under these circumstances, there are two velocity distributions (or any combination of them) that enable a vortex array to move as a unit without changing in shape as time progresses. These two motions are illustrated in Fig. 2 as uniform motion in rotation and in translation. Consideration is first restricted to the initial motion of the flat sheets and no specification is made as to the stability of the motion of the vortex distribution. The two-dimensional point vortices are

Fig. 2

assumed to have their axes nearly aligned with the x or streamwise direction (see Fig. 1 for coordinate system) so that the velocity components at time $t = 0$ can be taken as[†]

$$v_i)_{t=0} = 0 \quad (1a)$$

$$w_i)_{t=0} = \sum_{j \neq i}^N \frac{\gamma_j}{2\pi(y_i - y_j)} = \begin{cases} \Omega y_i & \text{for rotation} \\ w_0 & \text{for translation} \end{cases} \quad (1b)$$

$$(1c)$$

where v and w are the velocity components in the y and z directions, γ_j is the strength of the j th vortex, and N is the number of vortices in the array. For convenience, the vortices are assumed to be spaced uniformly along the y axis at $t = 0$. Since the location and velocity are known for every vortex in the array, and the vortex strengths are unknown, a sequence of equations can be written using Eqs. (1). The resulting matrix of equations can be inverted numerically on an electronic computer to yield the strengths of the vortices.[‡] The span-load distribution that corresponds to one of these arrays is found by summing the vortices from one end or the other, as appropriate, to achieve

[†]The use of vortices with artificial viscous cores (as suggested by Chorin and Bernard¹² and by Kuwahara and Takami¹³) instead of the potential vortices used here stabilizes and smooths out the vortex motion. It does not alter the qualitative nature of the solutions, however, if the core radius is less than the initial vortex spacing. Since the character of these calculations is not greatly different, the viscous core results are not included.

[‡]The subroutine used to invert the matrix is an improved double-precision linear equation solver developed by Richard T. Medan of the Ames Research Center.

realistic loadings. That is, the relationship

$$\gamma(y) = -d\Gamma(y)/dy \quad (2)$$

yields

$$\Gamma_{i+1}(y_{i+1} + \delta/2) = \Gamma_1(y_1 - \delta/2) - \sum_{j=1}^i \gamma_j(y_j) \quad (3)$$

where $\Gamma(y)$ is the circulation which is proportional to the span loading and $\Gamma_1(y_1 - \delta/2)$ is the circulation at the end of the array at which the summation begins. The circulation Γ_1 is taken as zero if it corresponds to a wingtip and to Γ_Q if it corresponds to the inboard end of the array. The spacing of the vortices given by $\delta = y_{i+1} - y_i$ will be related to the span b through the number of vortices used to represent the vortex sheet shed by the entire wing.

Motion of Vortex Arrays

The vortex arrays designed in the previous section will move initially in either rotation or translation. If the boundary conditions are such that the array elements are never disturbed and the calculations are free from numerical error, the arrays would move as specified for an indefinite period. Since, in practice, flow disturbances will always be present, this section considers the motion of the elements in the arrays for various span loadings on wings when the hypothetical flow conditions are not met and the subsequent time-dependent motion is not uniform. That is, an estimate is made of the sheet motion downstream of the wing trailing edge under conditions that are not ideal. The purpose of these calculations is to find out whether the vortex arrays are stable or unstable and whether the sheet rolls up, breaks up, and how it moves when it is disturbed by certain assumed flow

nonuniformities. These results will indicate whether rollup has been eliminated, suppressed, or not appreciably altered when the span loadings are built around the uniformly rotating and translating arrays derived in the previous section.

Before presenting the results for the various cases, the method used to calculate the motion for $t > 0$ the vortices in the arrays is discussed. As illustrated in Fig. 1, at $t = 0$ the vortex sheets are assumed to be flat (no dihedral) and to lie on the y axis. The semi-infinite length of the vortices in the x direction (i.e., from the lifting line at $x = 0$ to $x = \infty$) and the resulting reduction in the induced velocities near $x = 0$ is ignored. Any influence of a fuselage, tail, etc. on the vortex motion is also assumed to be negligible. The expressions used here for the general motion of the vortices are then those for two-dimensional potential vortices.[†]

$$v_i = \frac{\Delta y_i}{\Delta t} = - \sum_{j \neq i}^N \frac{\gamma_j (z_i - z_j)}{2\pi [(y_i - y_j)^2 + (z_i - z_j)^2]} \quad (4a)$$

$$w_i = \frac{\Delta z_i}{\Delta t} = + \sum_{j \neq i}^N \frac{\gamma_j (y_i - y_j)}{2\pi [(y_i - y_j)^2 + (z_i - z_j)^2]} \quad (4b)$$

The locations of the N vortices at an advanced time were found by using velocity averages over the time increment Δt . Since the final positions of the vortices affect the calculated velocities, it was necessary to iterate about five times for the new locations. In order to obtain an estimate of any numerical errors that may be growing during a calculation, the Kirchhoff-Routh path function¹⁴ Wr was monitored, where

$$Wr = \sum_{i=1}^N \sum_{j=i+1}^N \left(\frac{\gamma_i \gamma_j}{2\pi} \right) \ln r_{ij} \quad (5)$$

and r_{ij} is the distance between the i th and j th vortices. Since Wr should

remain a constant for a system of potential vortices, the calculations were terminated when the third significant figure (i.e., plotting accuracy) in Wr began to be affected by accumulated errors. The first and second moments of circulation for each side expressed as

$$\bar{y}\Gamma_{\mathcal{L}} = \bar{y} \sum_{i=1}^{N/2} \gamma_i = \sum_{i=1}^{N/2} y_i \gamma_i \quad (6a)$$

and

$$J = \sum_{i=1}^{N/2} [(y_i - \bar{y})^2 + (z_i - \bar{z})^2] \cdot \gamma_i \quad (6b)$$

were also monitored to see how they were altered by the sheet motion. Since the total circulation in the wake is zero, the centroid for the whole array is at infinity. Hence, the second moment J for each side might vary considerably during a calculation and therefore it is unreliable as an estimate for the accuracy of the numerical calculations. These techniques and the dimensionless quantities, $T = 4t\Gamma_{\mathcal{L}}/b^2$, $Y = 2y/b$, $Z = 2z/b$, $V = vb/2\Gamma_{\mathcal{L}}$, $W = wb/2\Gamma_{\mathcal{L}}$, and $GAM = \Gamma(y)/\Gamma_{\mathcal{L}}$, were used to generate the results which follow.

Vortex Wakes Consisting of Uniformly Rotating Arrays

Since the array that rotates uniformly consists of vortices all of the same sign, it can represent the vortex wake shed by only one side of the wing. A second array identical in all respects but opposite in sign must then be used to represent the vortex wake shed by the other half of the wing. The space allowed between the two arrays is arbitrary and that part of the span has uniform loading at the center line value. Since each array can occupy part or all of the semispan by allowing the gap to be small or large, the wing planform, twist, or camber could be considered to be tailored over a certain percentage of the span to produce a rotating array from each half of

the wing. That is, a wing tailored 40% would shed a vortex sheet from the outer 40% of each side of the wing. The strength of each sheet would be such that it would rotate as a unit if the sheet from the other wingtip did not interfere. Since the two sides do influence the motion of the arrays, the motion of one array is first presented in Fig. 3 to illustrate the hypothesized character of the vortex motion. Since no disturbances are present, the vortex array rotates as expected. The results are shown in Fig. 4 for a case wherein two rotating arrays, opposite of the sign, are added to form a complete span loading for a wing tailored 90% of its span. The induced velocities for the vortices or downwash, $W = w(y)/U_\infty$, and the streamlines for the $x = 0$ plane are included to illustrate how they differ from those for an elliptically loaded wing (compare with Fig. 12). It is seen in Fig. 4c that the two vortex arrays interact enough to destroy the uniform rotation postulated. If the initial position of a vortex is displaced from the y axis, as shown in Fig. 5, the orderly part of the rotation is destroyed sooner. In both of these cases, the sheet from a side apparently does not roll up into a single, well-organized vortex; roll up therefore appears to have been suppressed but not eliminated by span loadings built around vortex arrays designed to rotate as a unit. The final disposition of the vortices shown in Figs. 4c and 5 appears not to be sensitive to disturbances.

Fig. 3

Fig. 4

Fig. 5

As the gap between the two sheets is increased from 10% of the span, the two arrays rotate more independently; however, the vorticity is then concentrated over a smaller part of the span, resulting in more intense vortex cores. It was thought that the breakup of the sheet might be delayed further into the wake by specifying a triangular downwash along the wing at $t = 0$. As a result, the initial motion was improved slightly but later

motions were not as orderly as when the two sides were designed independently of one another.

The induced drag for wings with various amounts of tailoring is presented in Fig. 6 where the value for an elliptically loaded wing ($C_{D_i} = C_L^2/\pi AR$) is used as the reference. An induced drag penalty occurs when these tailored loadings are used if the comparison is made on the basis of span efficiency. However, Jones¹⁵ has pointed out that the span load distribution is approximately triangular for maximum efficiency when the lift and wing root bending moment (rather than span) are held constant. Jones then suggests that lift efficiency based on span may not always be the proper criteria because loadings other than elliptical may be more desirable if there are other advantages to a particular loading, such as vortex hazard alleviation and minimum root bending moment.

Fig. 6

The tailored span loadings can be achieved by planform shape, by wing twist or camber, or by the use of flaps. Figure 7 presents the planforms estimated to provide loadings tailored 40% and 90% when the wing is flat. These shapes were derived by making the local chord of such a length that the specified loading is obtained in the presence of the local upwash or downwash and the spanwise transfer of lift is ignored (i.e., strip theory). In equation form, the chord $C(Y) = c(y)/c_{CL}$ is given by

Fig. 7

$$C(Y) = GAM(Y) [AR + W(0) (dC_L/d\alpha)] / [AR + W(Y) (dC_L/d\alpha)] \quad (7)$$

where $W(Y) = w(y)/U_\infty$. The tips of the tailored wings shown in Fig. 7 resemble the ogee tip design of Ward;^{3,9} this design reduces the velocity in the vortex cores shed by the tips of helicopter rotor blades in an effort to reduce the noise.

When the number of vortices in the array representing a sheet is allowed to increase indefinitely, the vorticity distribution is given by

$$\gamma(y) = -[(d\Gamma(y)/dy)] = \pm(4\Gamma_0/\pi b)[1 - (2y/b)^2]^{1/2} \quad (8a)$$

and the circulation is

$$\Gamma(y) = \Gamma(-b/2) + (\Gamma_0/\pi) \left\{ (2y/b) [1 - (2y/b)^2]^{1/2} + \sin^{-1}(2y/b) + \pi/2 \right\} \quad (8b)$$

where Γ_0 is the total circulation in the sheet. These two functions are noted to be the limiting form of the elliptic volume distribution derived by Lamb¹⁶ (p. 232) to rotate as a unit, and studied by Kuwahara, and Takami¹³ using discrete vortices.

The foregoing representation for the rotating array, Eq. (8), can also be represented by the usual Fourier series representation used in the analysis of span load distributions (e.g., Glauert,¹⁷ p. 38) wherein the substitution $y = -(b/2)\cos \theta$ is made. The downwash $w(y)$ and circulation $\Gamma(y)$ are usually given in series form as

$$w(\theta) = U_\infty \sum_{n=1}^{\infty} nA_n \frac{\sin n\theta}{\sin \theta} \quad (9a)$$

$$\Gamma(\theta) = 2bU_\infty \sum_{n=1}^{\infty} A_n \sin n\theta \quad (9b)$$

It is incorrect to assume that a purely linearly varying downwash is obtained with Eq. (9a) if all terms are zero except A_2 . The bound circulation $\Gamma(\theta)$ then consists of only the $\sin 2\theta$ term, which is not enough; that is, $\Gamma(y) \neq 2\Gamma_0 y \sqrt{1 - (2y/b)^2}/\pi b$. The correct series expansion in θ is obtained from Eq. (8b) as

$$\Gamma(\theta) = \Gamma(-b/2) + (\Gamma_0/\pi) [\theta - (\sin 2\theta/2)]$$

which becomes

$$\Gamma(\theta) = \Gamma(-b/2) + (\Gamma_o/2\pi) \left[\pi - \sin 2\theta - 2 \sum_{n=1}^{\infty} (\sin 2n\theta/n) \right] \quad (10)$$

The solution Eq. (8b) for the rotating array makes it possible to calculate the structure of a fully-developed vortex by Betz' theory in closed form. By Eq. (17) of Ref. 11, the radius which contains a given amount of circulation is given by

$$2r_1/b = |\bar{Y}_1 - Y_1| = \left| \int_0^{Y_1} [\Gamma(Y) - \Gamma(0)] dY / \pi [\Gamma(Y_1) - \Gamma(0)] \right|$$

or, by Eq. (8b)

$$2r_1/b = Y_1 - 2\Gamma_o [(1 - Y_1^2)^{1/2} - 1] / \{3\pi [\Gamma(Y_1) - \Gamma(0)]\} \quad (11)$$

where $Y_1 = 4\{y - [1 - (T_t/2)](b/2)\} / T_t b$ and T_t is the fraction of the wing that is tailored. The circulation $\Gamma_v(r_1)$ contained in the vortex at the radius r_1 is then

$$\Gamma_v(r_1) = 2\Gamma(Y_1) \quad (12)$$

because the vortex sheet rolls up about its center. The center of the vortex is located at the spanwise location of the center of the tailored wing segment because that is the centroid of vorticity for a side. The circumferential velocity is given by

$$v_\theta = [\Gamma_v(r_1) / 2\pi r_1] \quad (13)$$

The various results for such a rollup is presented in Fig. 8, where the velocity components are shown only for the part of the flow field containing vorticity. Outside of this region, the velocity falls off as $1/r$.

Fig. 8

Vortex Wakes Consisting of Uniformly Translating Arrays

An array of equally spaced vortices on a straight line that is designed to translate as a unit makes up the wake of a complete span loading, i.e.,

both sides of the wing. A gap could be designed into the center of the array to yield a uniformly loaded center section, but this case will not be discussed here. Hence the only variables to be considered are the number of vortices and the type of disturbance assumed to perturb the motion of the arrays. The motion of such a sheet of vortices and the shape of the vortex lines for an array of 20 vortices are shown in Fig. 9. Presented in Fig. 10 are the vortex paths when the initial position of a vortex is perturbed a small amount. The orderly translation of the array is seen to break up quickly into a random motion that destroys any orderliness of the wake.⁵ This randomness suggests that the vortex wake behind such a lifting surface might dissipate rapidly so that it would become nonhazardous at a distance not too far behind the generating aircraft. The random locations of the vortices also suggest that the net rolling moment on an encountering aircraft would be greatly reduced from those cases wherein the vortex system is organized into an orderly spiral rollup. This seemingly random motion appears to arise from the fact that two vortices of opposite sign and of unequal magnitude form a pair. That combination then moves along a path whose radius of curvature R is governed by the velocity induced by the two vortices on each other,

$$R = d(\gamma_{\ell} - \gamma_r) / [2(\gamma_{\ell} + \gamma_r)]$$

where d is the distance between the two vortices and γ_{ℓ} and γ_r are the strengths of the left and right vortices, respectively. The orbits of the various pairs of vortices are also governed by the rest of the vortices in the wake, but the proximity of any two produces a gross motion that is dependent largely just on the two vortices that have paired off. The magnitude

⁵The use of an artificial viscous core in the vortex structure suppresses the excursions but the random character persists.

and type of disturbance influence how the vortices are matched to produce what appears to be random motion. Since the uniform translating motion was destroyed by a small perturbation, there is little doubt that disturbances of sufficient magnitude exist behind the generating aircraft in actual flight to cause the vortex array to go into the random motion predicted theoretically if stepped loadings can be generated. An estimate of the induced drag for these loadings was not made because of the discontinuous character of the loadings.

In the previous subsection a closed form solution was presented for the rotating array when the number of vortices N became infinite. A similar result could not be found for the array that translates as a unit because the amplitude of the steps in the vortex strengths decreases only slightly as N increases (see Fig. 11). The transition to an infinite number of vortices  Fig. 11 apparently does not result in a smooth loading. However, a continuous loading is achieved if two arrays equal in number and in strength are superimposed on one another so that one array is offset from the other by one vortex spacing. The loading is then elliptical with the characteristic downwash velocity being uniform everywhere except at the two ends, where it is discontinuous. Figure 12 presents the calculations for such a sheet. As expected, rollup proceeds  Fig. 12 rapidly and orderly from the wingtips inboard. If an initial disturbance is given to such an array, the rollup proceeds almost unchanged, illustrating why it is so hard to break up vortices produced by span loadings that are nearly elliptical.

Vortex Wakes Using Combinations of Span Loadings

Although advantages may be achieved in reducing the wake vortex hazard by use of the span loadings introduced in the previous sections, one may ask

whether the concepts derived can be applied to current aircraft configurations. For example, the exact values needed to generate a uniformly translating array will be difficult to produce in practice. However, it may be possible to use leading- and trailing-edge flaps to generate a span loading that approximates the specified one so that a random motion of the vortices is still obtained. Also, a large number of elements may not be needed to produce enough randomness in the wake to render it much less hazardous. These possibilities are now studied by first combining the two foregoing special arrays with each other to generate another class of loadings. After an approximation to the stepped loading is studied, it is then applied to the span loading of a current aircraft.

Combination of Rotating and Translating Arrays

If the span loading for an array that rotates uniformly is added to one that translates as a unit, the question arises as to what proportion of each should be used in the mixture to develop a particular result. Since the objective is to discover possible practical loadings or vortex wakes that produce nonhazardous wakes, the combination desired is the one that most closely approximates current span loadings but yet has the desired properties of a randomized wake vortex system. Because a stepped loading of large magnitude and containing many elements is effective but difficult to produce in practice, the best combination is the one that produces a random wake with fluctuations in the span loading that are minimal in number and magnitude. Therefore, a sequence of computer runs were made in which the proportion of stepped loading (i.e., translating array) was gradually increased until a somewhat random wake was achieved in the 90% tailored case. Figure 13 presents the case for 40 vortices wherein more than enough of the stepped loading

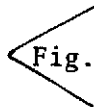


Fig. 13

has been added to produce an apparently randomized wake in the tailored loading (rotating array). The steps in the span loading shown are not as large as the stepped loading by itself. If the number of vortices in the array is reduced below 40, the magnitude of the steps must be increased.

Sawtooth Loading

The magnitude of the vortex strengths in the array that translates as a unit have up to now been calculated precisely and used in this form. Since such precision is difficult to achieve in experiments and since the loading to a first approximation is simply an elliptic loading plus the loading of an array of vortices equal in magnitude but alternating in sign, it may be possible to get the randomizing influence with an array wherein the vortices are all equal in magnitude but alternate in sign. The span loading and the vortex motion that result from such an array are presented in Fig. 14. As expected, the wake becomes random and rollup does not occur. For convenience, this array (i.e., with vortices equal in magnitude but alternating in sign) is referred to as sawtooth loading, whereas that of the translating array is called the stepped loading. Furthermore, randomization of the vortex wake again occurs when a sawtooth loading is added in the same proportion as the stepped loading to the 90% tailored loading. The proportion of stepped or sawtooth loading required to randomize the wake vortex system of a given span loading is not necessarily a well defined amount; rather, the randomness seems to increase rapidly after the sawtoothing has increased above a certain amount or fraction of the centerline circulation.

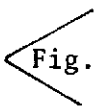


Fig. 14

Combination of Sawtooth with Aircraft Loading

The concepts generated in the previous sections can now be tried on a span-load distribution typical of current large aircraft. The span load and resulting motion of the vortices in the wake are illustrated in Fig. 15a and b for a landing configuration. Note that fluctuations already exist in the loading as a result of the arrangement used for the flaps and pylons during landing. These built-in variations, however, need to be supplemented with other spanwise variations to achieve sawtooth loading that is effective in randomizing the wake. As the proportion of sawtooth loading is increased, the wake system progresses from an orderly rollup into the somewhat random system shown in Fig. 16. A greater proportion of sawtoothing and a greater number of segments would of course produce a more chaotic wake. The loading that can be achieved with a given wing flap system will determine the amount and the frequency of the sawtooth loading. It will then be necessary to try various combinations of flap settings to see the kinds of loadings that are possible and then to calculate the vortex wake to determine which configuration produces the least hazardous wake.

Fig. 15a
Fig. 15b

Fig. 16

Concluding Remarks

The two hypothetical vortex arrays introduced and studied in this paper were found not to roll up as postulated, but the motion of individual elements was found to be unstable to disturbances. The breakup of the uniform rotation of the array first considered leads to a vortex wake that rolls up into several vortices per side instead of the two well-organized, tightly bound vortices found behind wings of approximately elliptic loading.

The random motions of the vortex elements behind a wing that sheds a disturbed, translating array of vortices suggest that such a wake would diffuse and decay rapidly when viscosity is present and would produce a small rolling moment on encountering aircraft. It was found that comparable results could also be achieved with an array consisting of vortices that are equal in magnitude but which alternate in sign. This observation indicates that random motion can probably be achieved with a variety of stepped loadings. The addition of these rapidly varying loadings to existing span loadings might be a method for reducing the hazard to small aircraft entering the wake of large aircraft. It remains to be shown with ground-based experiments, however, that sufficient variations can be generated in the span loadings with flaps, slats, etc. to produce in the wake the disorganization predicted theoretically. These results then indicate that the wake behind an aircraft can be made less hazardous by reducing the gradient in the loading at the wingtip and by making several rapid changes in the span loading to produce several vortices that move about somewhat randomly; in this way, the usual two intense well-organized vortices are avoided.

References

- ¹ Corsiglia, V. R., Jacobsen, R. A., and Chigier, N., "An Experimental Investigation of Trailing Vortices Behind a Wing with a Vortex Dissipator," *Aircraft Wake Turbulence*, edited by John H. Olsen, Arnold Goldburg and Milton Rogers, Plenum Publishing Corp., New York, Sept. 1970.
- ² Bilanin, A. J. and Widnall, S. E., "Aircraft Wake Dissipation by Sinusoidal Instability and Vortex Breakdown," AIAA Paper 73-107, Washington, D.C. 1973.
- ³ Rorke, J. B., Moffitt, R. C., and Ward, J. F., "Wind Tunnel Simulation of Full Scale Vortices," A.H.S. Preprint 623, 28th Annual National Forum of the American Helicopter Society, Washington, D.C., May 1972.
- ⁴ El-Ramly, Z., "Aircraft Trailing Vortices - A Survey of the Problem," Technical Report ME/A 72-1, Nov. 1972, Carleton University, Ottawa, Canada.
- ⁵ Takami, H., "A Numerical Experiment with Discrete-Vortex Approximation, with Reference to the Rolling up of a Vortex Sheet," Sudaer No. 202, (AFOSR 64-1536), Sept. 1964.
- ⁶ Scheiman, J. and Shivers, J. P., "Exploratory Investigation of the Structure of the Tip Vortex of a Semispan Wing for Several Wing-Tip Modifications," TN D-6101, Feb. 1971, NASA.
- ⁷ Clements, R. R. and Maull, D. J., "The Rolling up of a Trailing Vortex Sheet," *Aeronautical Journal*, Vol. 77, No. 745, Jan. 1973, pp. 46-51.
- ⁸ Rehback, C., "Numerical Study of the Influence of the Wing-Tip Shape on the Vortex Sheet Rolling Up," TT F-14, 538, Aug. 1972, NASA.
- ⁹ Rorke, J. B. and Moffitt, R. C., "Wind Tunnel Simulation of Full Scale Vortices," CR-2180, March 1973, NASA.

- ¹⁰ Brown, C. E., "Aerodynamics of Wake Vortices," *AIAA Journal*, Vol. 11, No. 4, April 1973, pp. 531-536.
- ¹¹ Rossow, V. J., "On the Inviscid Rolled-Up Structure of Lift-Generated Vortices," *AIAA Journal of Aircraft*, to be published.
- ¹² Chorin, A. J. and Bernard, P. S., "Discretization of a Vortex Sheet, with an Example of Roll-Up," College of Engineering Report FM-72-5, Nov. 1972, Univ. of Calif., Berkeley, Calif.
- ¹³ Kuwahara, K. and Takami, H., "Numerical Studies of Two-Dimensional Vortex Motion by a System of Point Vortices," *Journal of the Physical Society of Japan*, Vol. 34, No. 1, Jan. 1973, pp. 247-253.
- ¹⁴ Lin, C. C., "On the Motion of Vortices in Two Dimensions," No. 5, Applied Mathematics Series, The Univ. of Toronto Press, Toronto, Canada, 1943.
- ¹⁵ Jones, R. T., "The Spanwise Distribution of Lift for Minimum Induced Drag of Wings Having a Given Lift and a Given Bending Moment," TN 2249, Dec. 1950, NACA.
- ¹⁶ Lamb, H., *Hydrodynamics*, Dover Publications, New York, 1945.
- ¹⁷ Glauert, H. *The Elements of Aerofoil and Airscrew Theory*, Cambridge University Press, Cambridge, England, 1948.

FIGURE TITLES

- Fig. 1 Schematic diagram of relationship between span loading $\Gamma(y)$, vortex sheet, $\gamma(y)$, Trefftz plane, and final rolled-up vortex for one side.
- Fig. 2 Two vortex arrays designed to move as a unit without rolling up.
- Solid-body rotation; $w = \Omega y$.
 - Uniform downward velocity; $w = \text{constant}$.
- Fig. 3 Motion of a single vortex array designed to rotate as a unit.
- Spanwise loading and downwash velocity.
 - Sheet positions as time progresses.
- Fig. 4 Flow characteristics for span loading built with two arrays designed to rotate as a unit; 90% tailored.
- Spanwise loading and downwash velocity at $x = 0$.
 - Streamlines in Trefftz plane at $x = 0$.
 - Oblique view of vortex paths; $T_{\max} = 3.0$.
- Fig. 5 Oblique view of vortex paths when the initial position of the fifth vortex is displaced 0.02 units for the 90% tailored case shown in Fig. 4; $T_{\max} = 3.0$.
- Fig. 6 Induced drag of tailored loadings referred to elliptic loading.
- Fig. 7 Estimated planforms of flat, untwisted wings tailored for span loadings that shed rotating vortex sheets from outer portions of wing ($R = b^2/\text{area} = 6$).
- Loading tailored 40%.
 - Loading tailored 90%.
- Fig. 8 Structure of fully-developed vortex for sheet designed to rotate as a unit according to Betz' theory (see Ref. 11).
- Loading on right wing.

- b) Circulation as a function of radius in developed vortex.
- c) Circumferential velocity in developed vortex.

Fig. 9 Characteristics of span loading built with array designed to translate as a unit.

- a) Span loading compared with elliptic loading and downwash velocity of each vortex in the array.
- b) Oblique view of each half of vortex sheet at various times;
 $T_{\max} = 3.0$.
- c) Oblique view of shape of vortex lines; $T_{\max} = 3.0$.

Fig. 10 Vortex motion of translating array when initial position of fifth vortex is displaced $0.02 b/2$. Note how vortices form pairs that move along circular paths deviating occasionally to exchange mates;

$T_{\max} = 3.0$.

- a) Vortex paths in Trefftz plane.
- b) Oblique view of vortex lines.

Fig. 11 Amplitude of steps in loading at centerline of translating array as a function of the number of vortices in the array.

Fig. 12 Characteristics of span loading obtained by adding two translating arrays after shifting them one vortex spacing spanwise. This loading quickly approximates elliptic loading as the number of vortices N as increased.

- a) Span loading of the combined translating arrays shown as stepped curve compared with elliptic loading and velocity of vortices at $x = 0$. Note the two vortices at the ends of the array with greatly different velocities.
- b) Streamlines in Trefftz plane at $x = 0$.
- c) Oblique view of vortex paths; $T_{\max} = 3.0$.

Fig. 13 Characteristics of span loading obtained by combining a translating array with a rotating array. Translational velocity = $(0.3b/4)x$ rotational velocity.

- a) Span loading and velocity of vortices at $t = 0$.
- b) Oblique view of vortex paths; $T_{\max} = 3.0$.

Fig. 14 Characteristics of sawtooth loading formed by equal vortices that alternate in sign.

- a) Span loading compared with elliptic loading and downwash velocity of vortices at $t = 0$.
- b) Oblique view of vortices; $T_{\max} = 3.0$.

Fig. 15 Characteristics of loading typical of current large aircraft in landing configuration.

- a) Vortex array approximation to span loading.
- b) Oblique view of vortices; $T_{\max} = 3.0$.

Fig. 16 Characteristic of wake of loading in Fig. 15 when sawtooth array of $\Delta\gamma = 0.2 \Gamma_0$ has been added.

- a) Vortex array approximation to span loading.
- b) Oblique view of vortices; $T_{\max} = 2.6$.

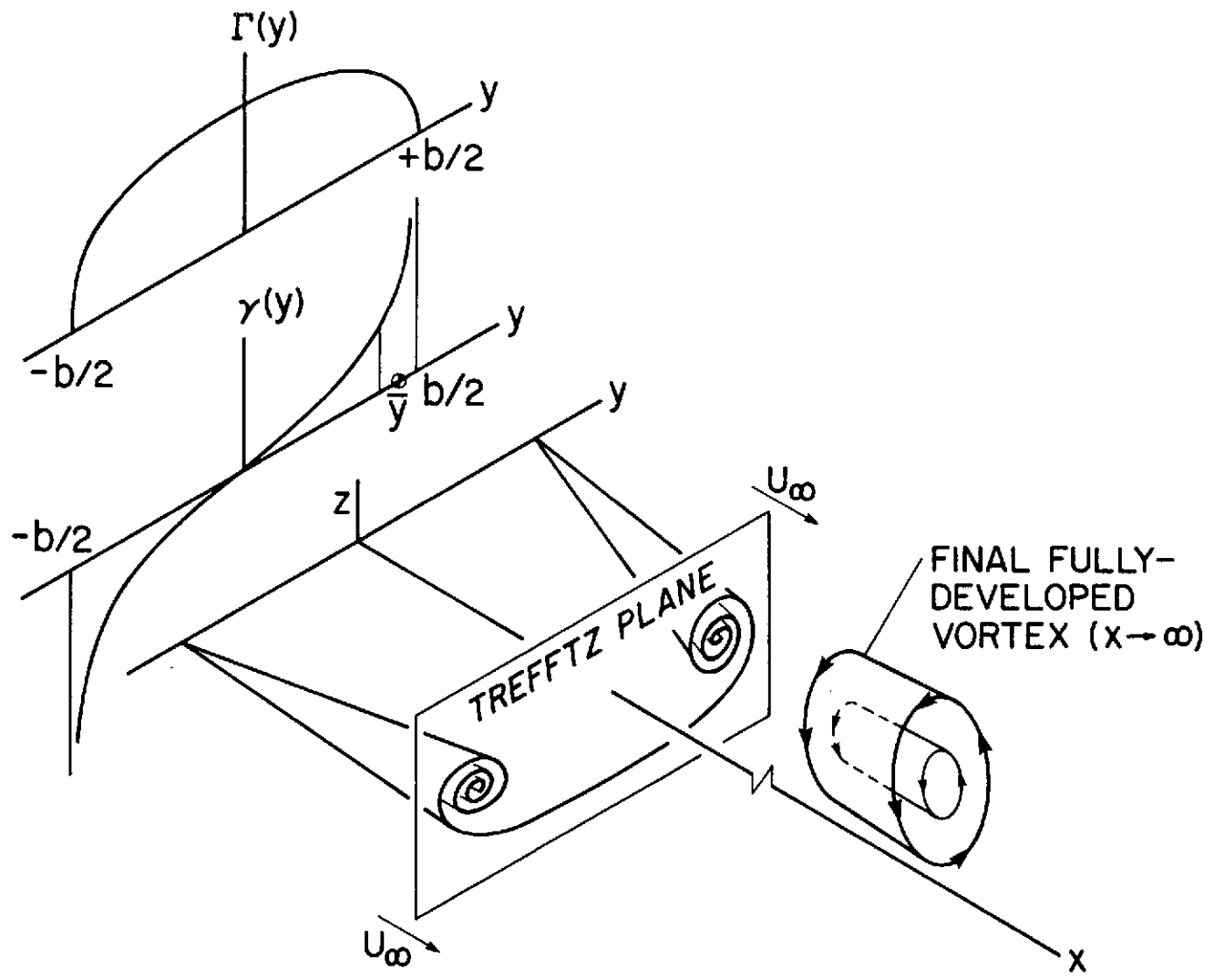


Fig 1

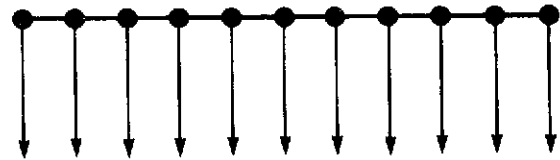
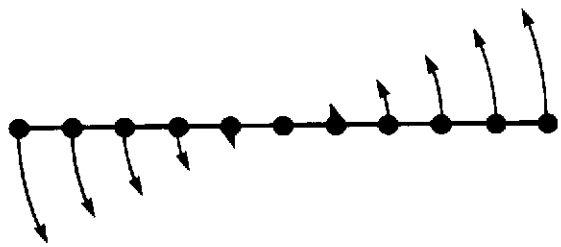


Fig. 2

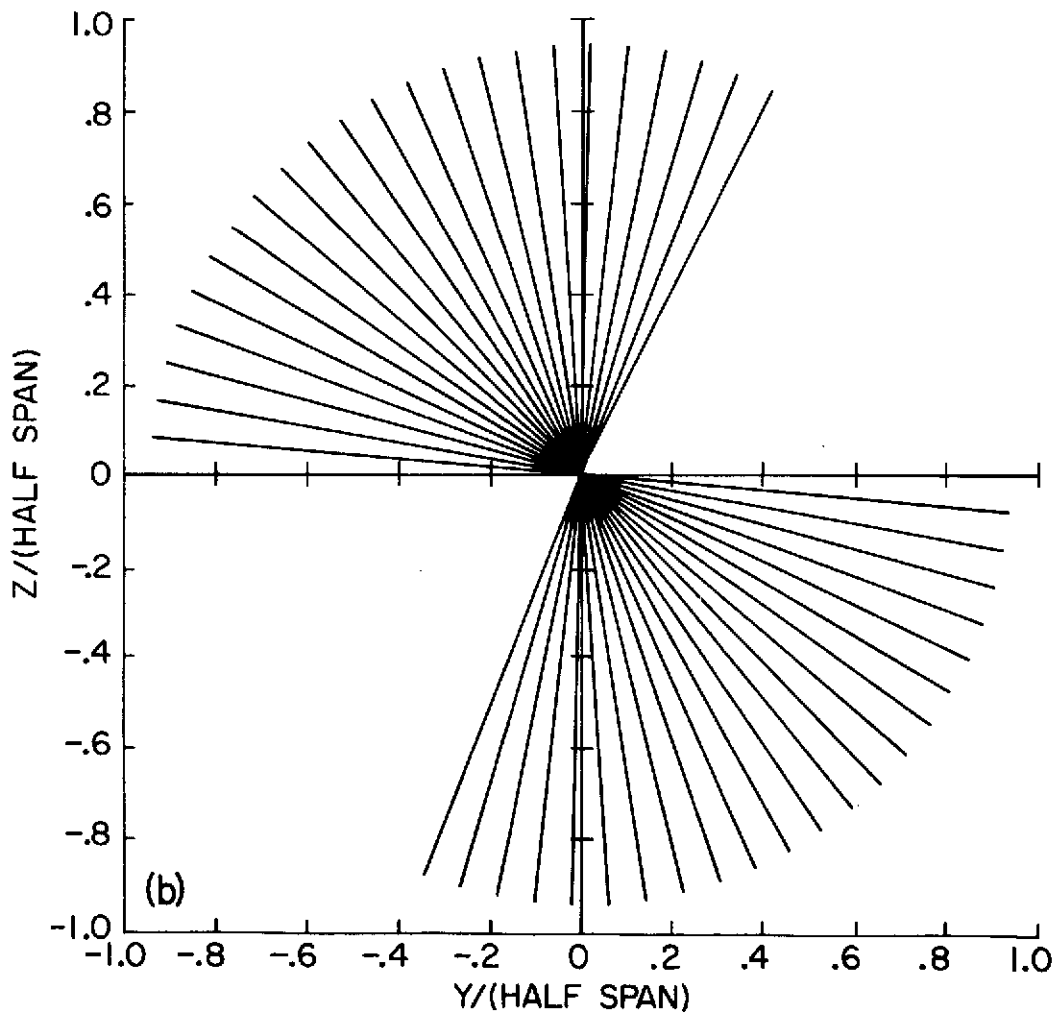
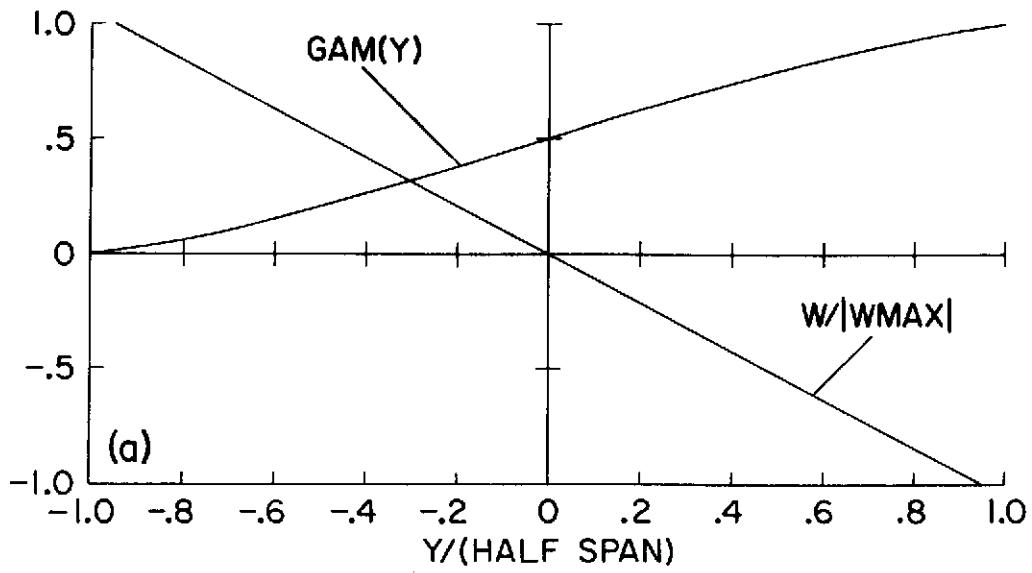
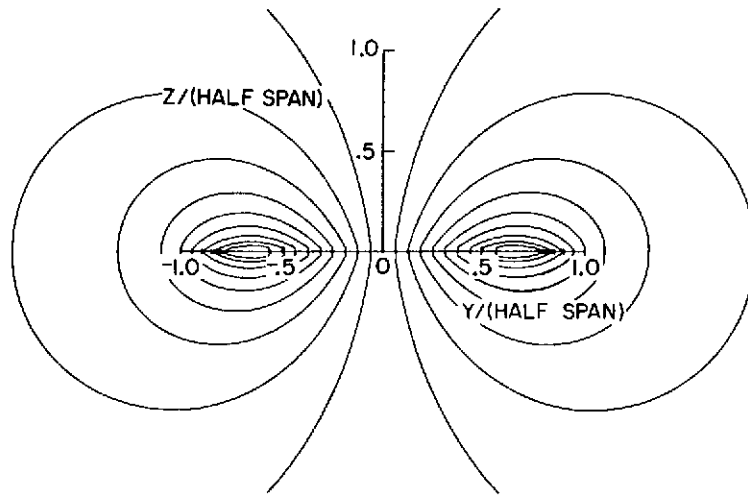
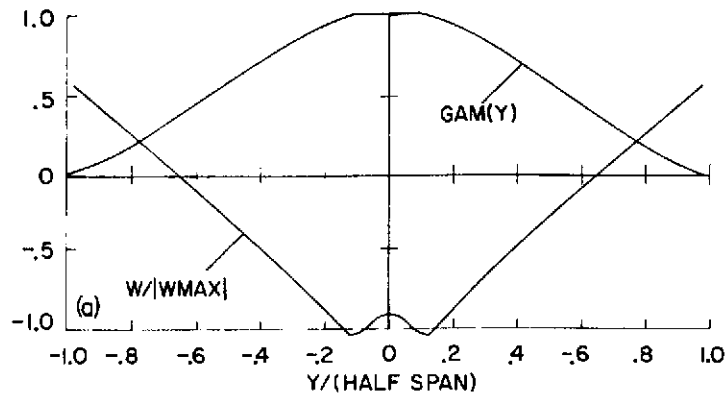
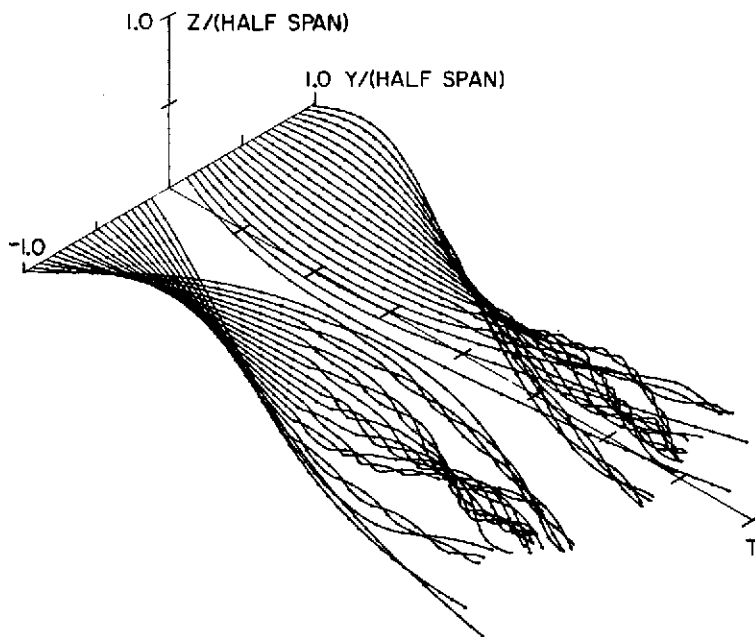


Fig. 3



(b)



(c)

Fig. 4

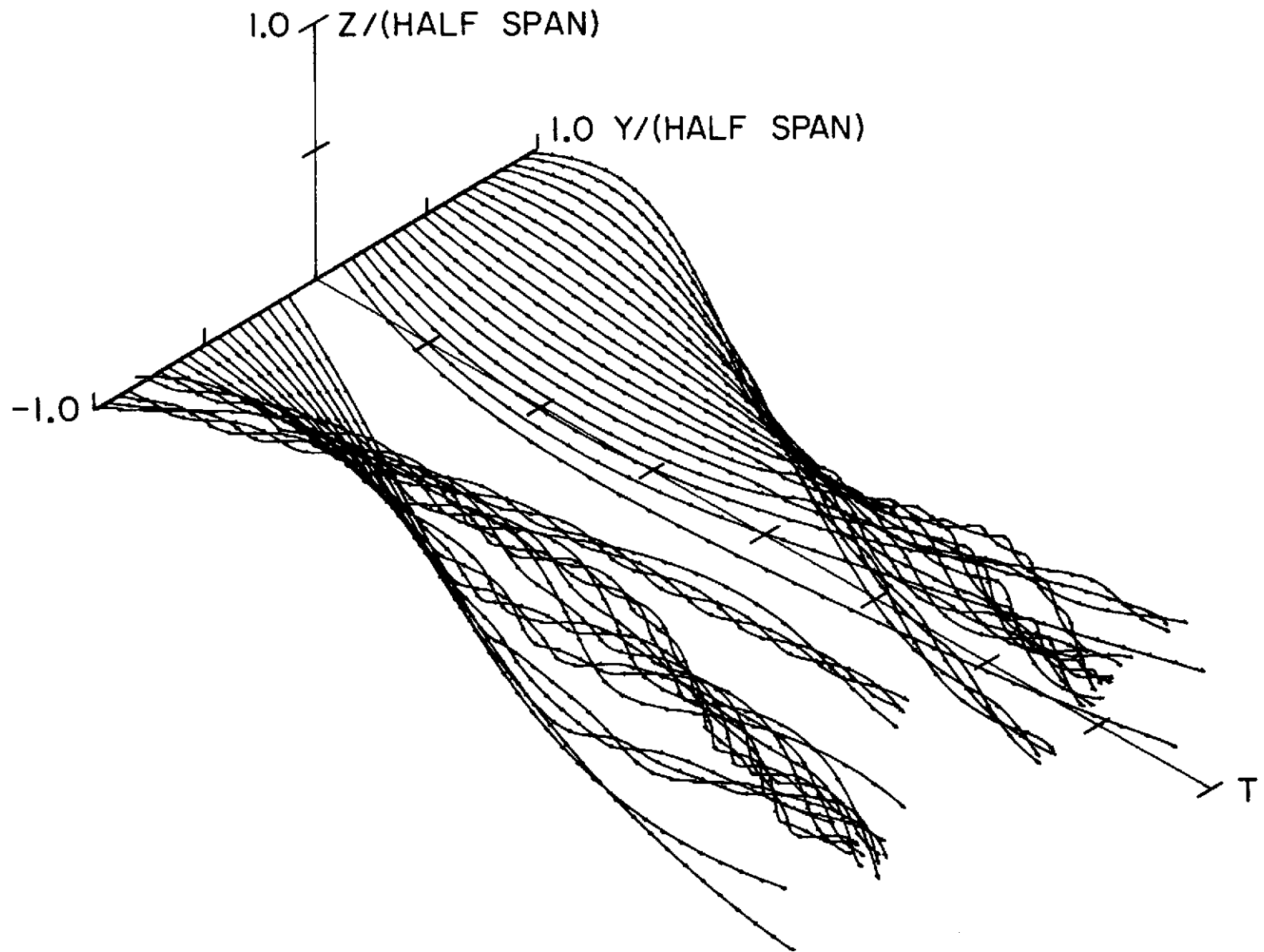


Fig. 5

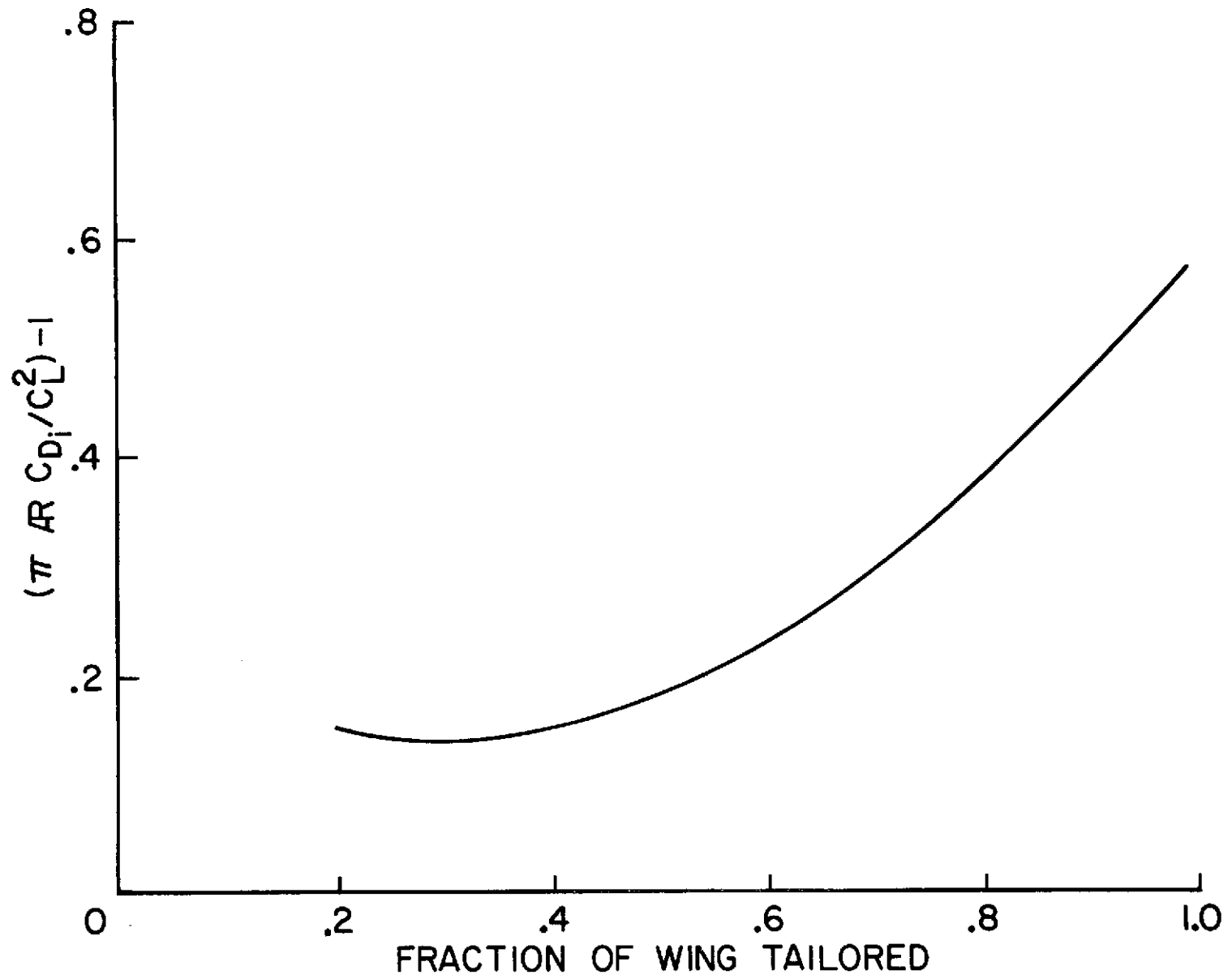
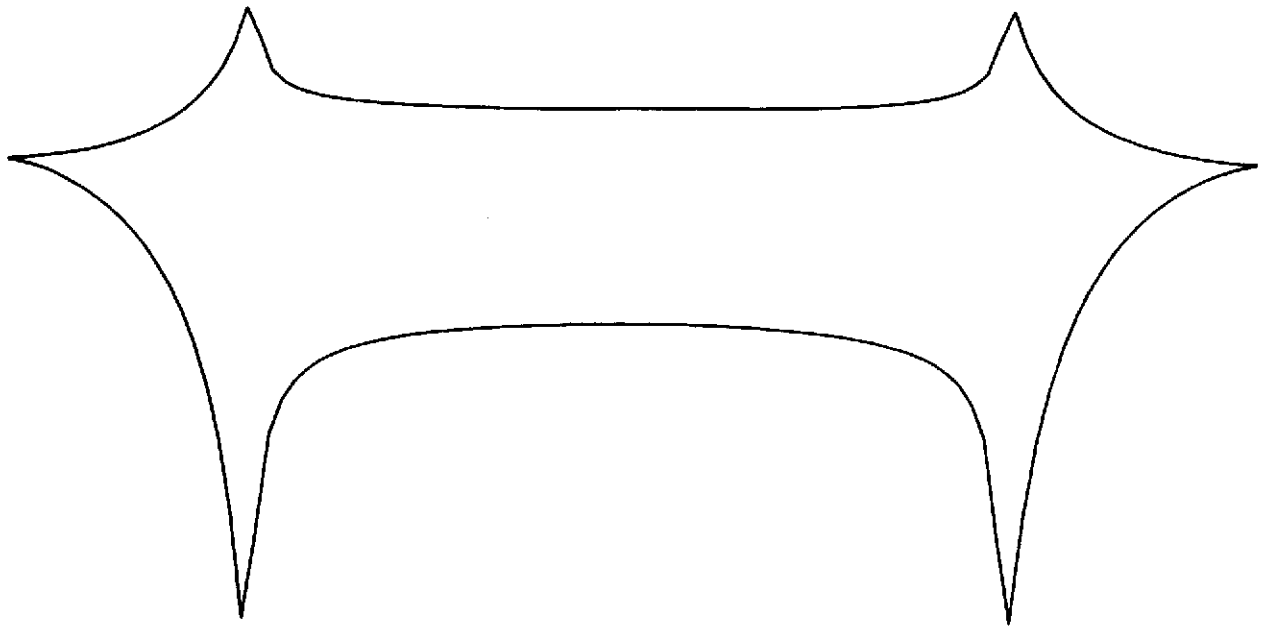
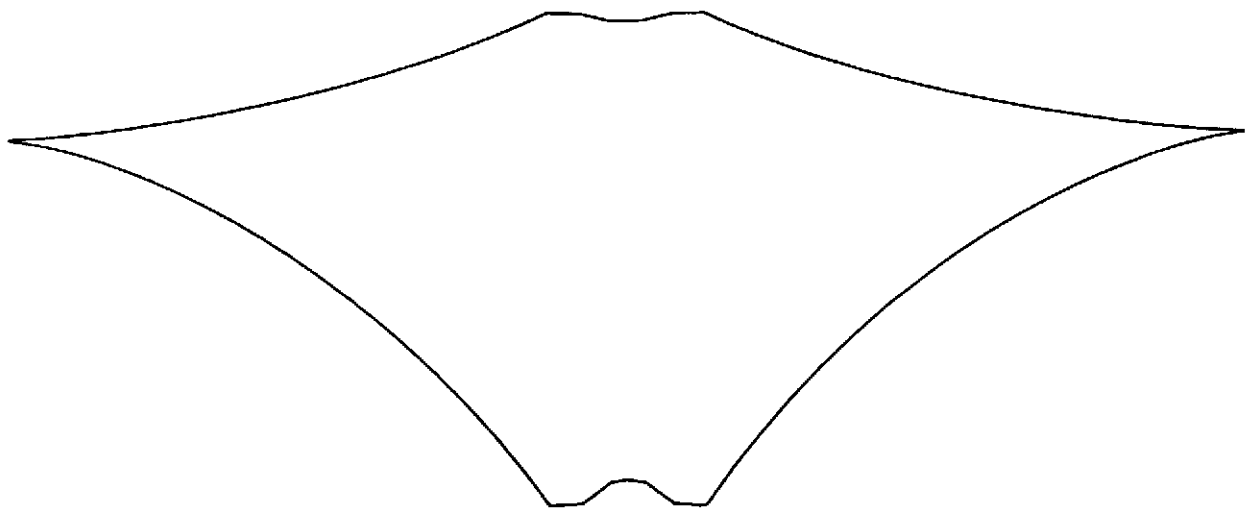


Fig. 6



(a) LOADING TAILORED 40%



(b) LOADING TAILORED 90%

Fig. 7

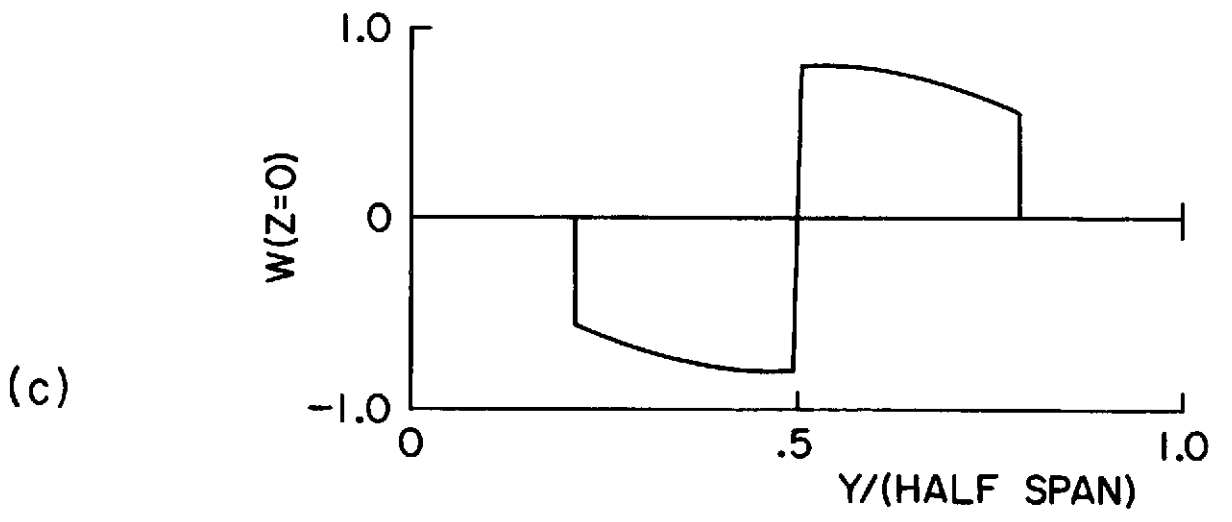
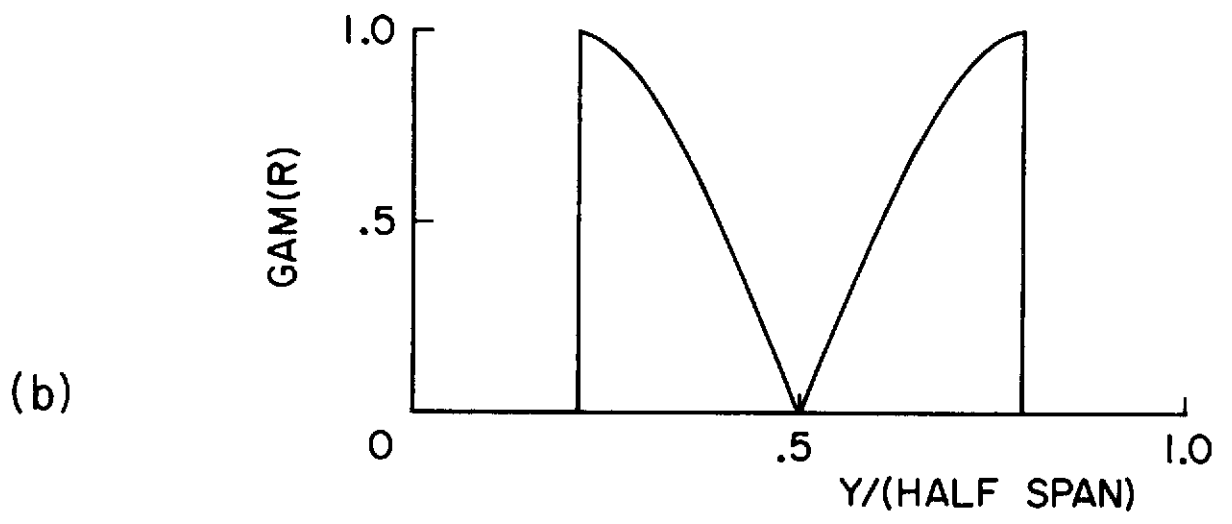
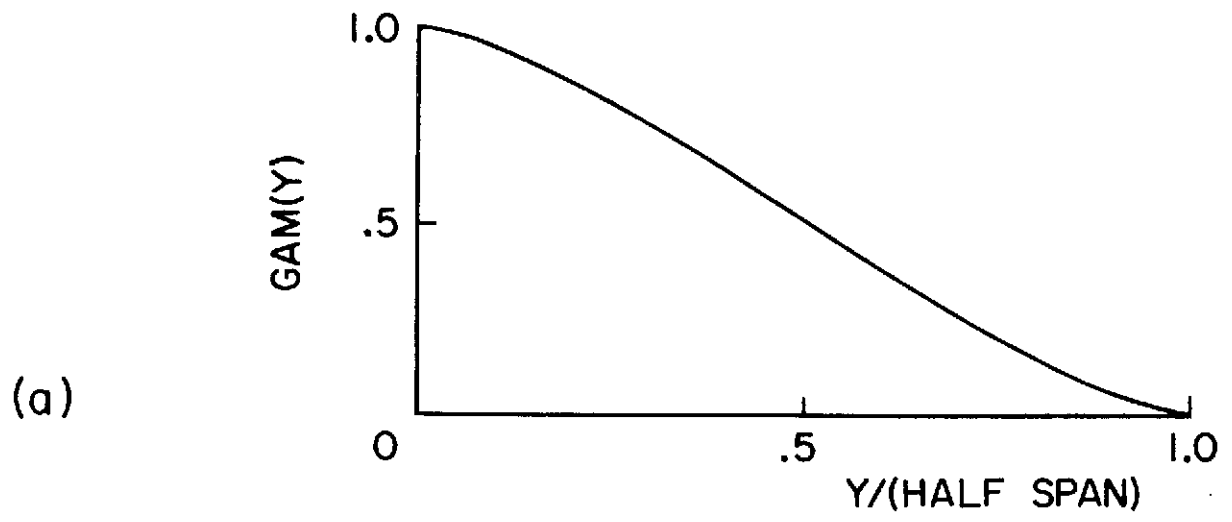


Fig. 8

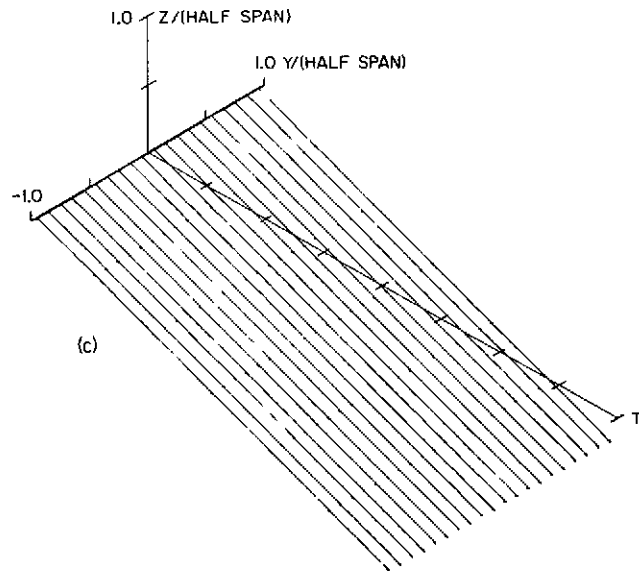
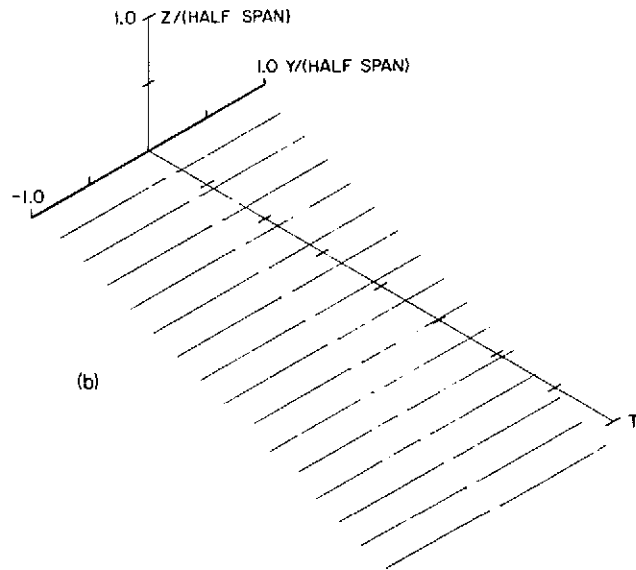
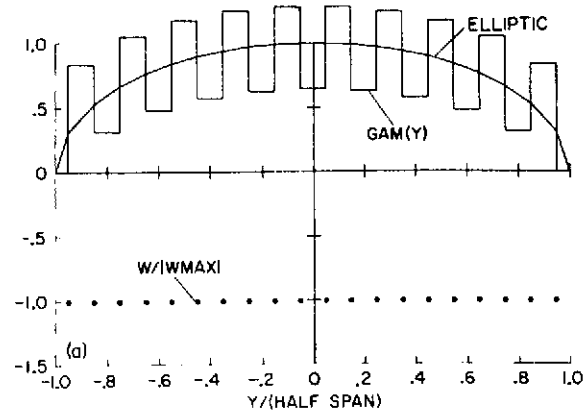


Fig. 9

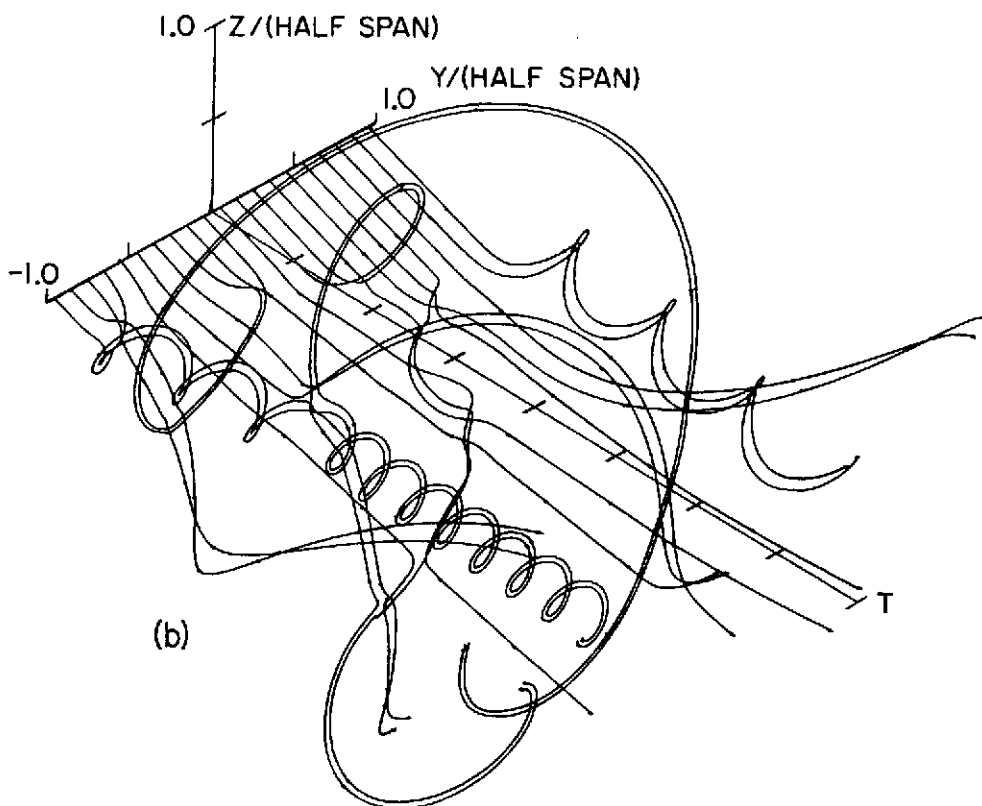
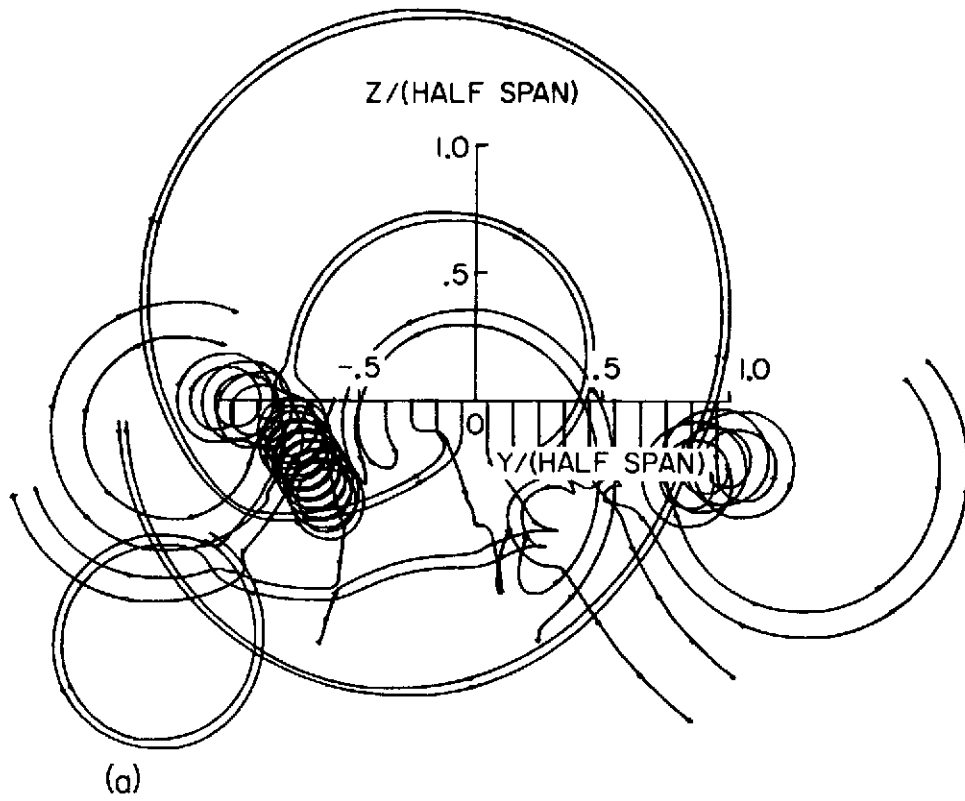


Fig. 10

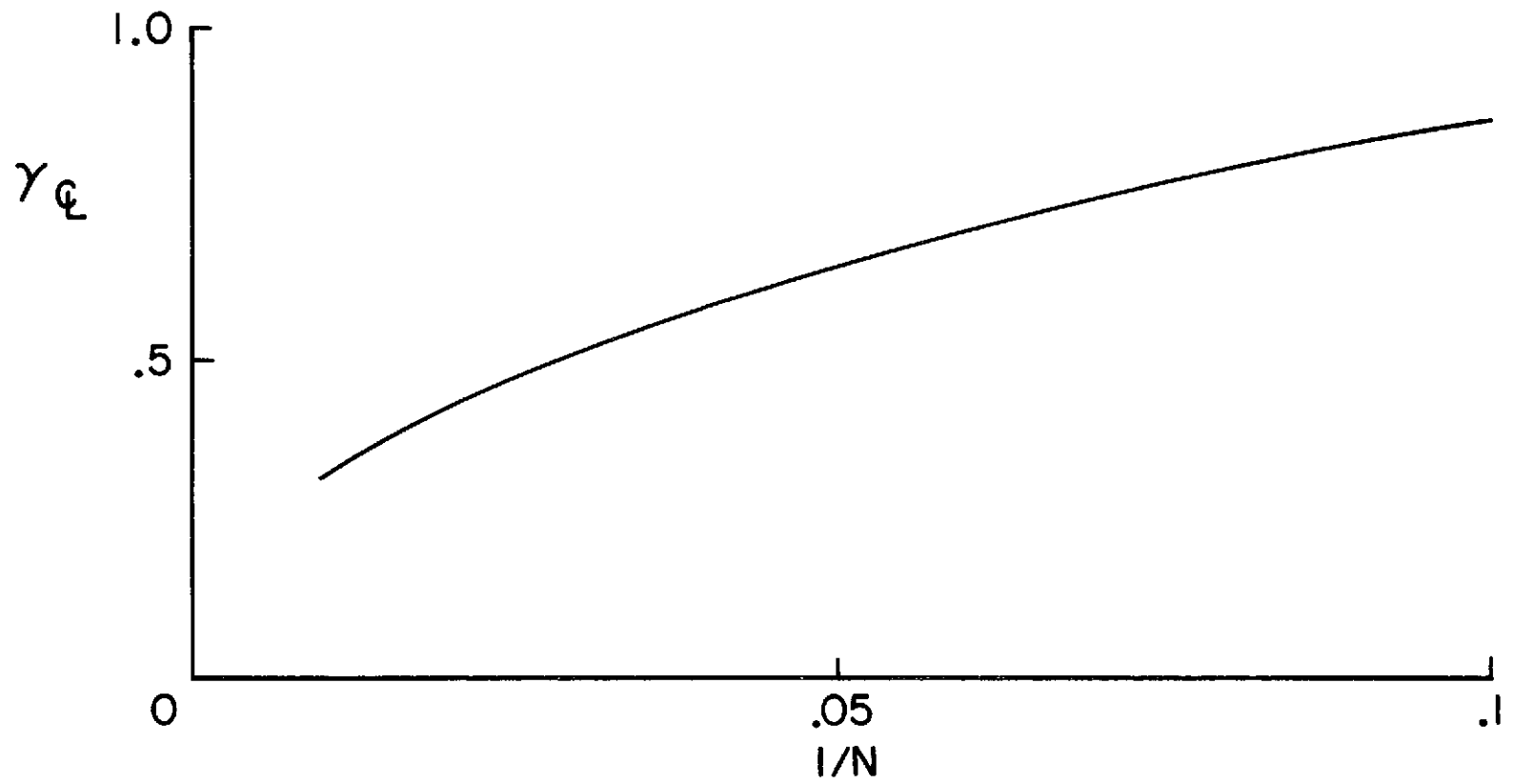


Fig. 11

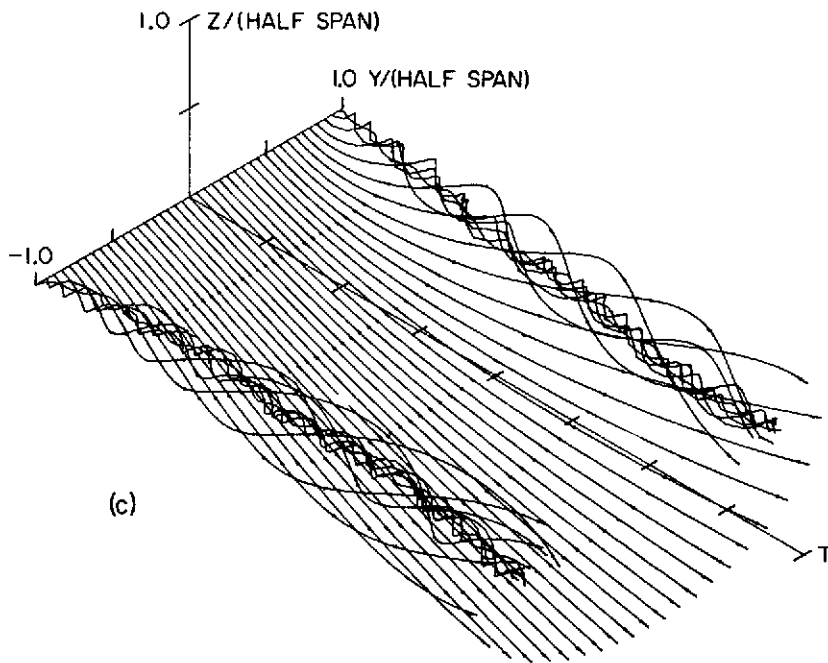
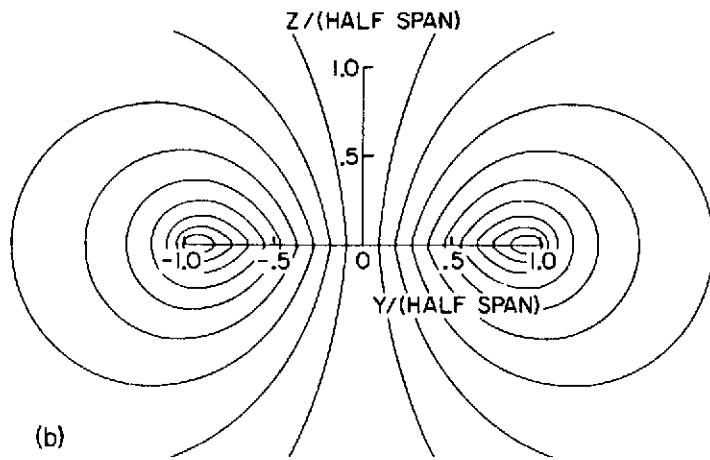
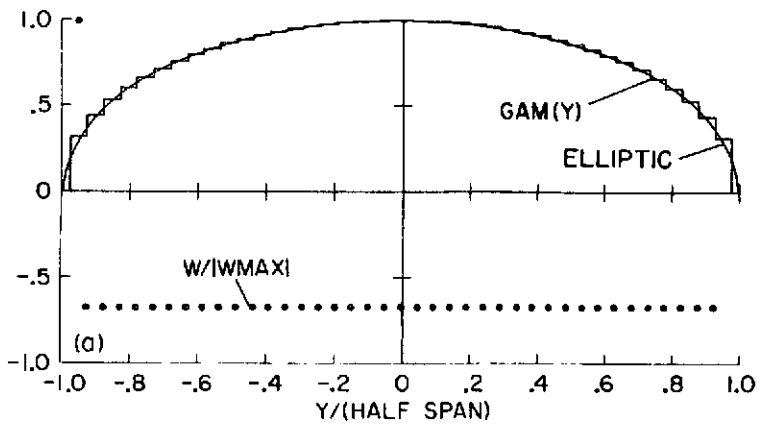


Fig. 12

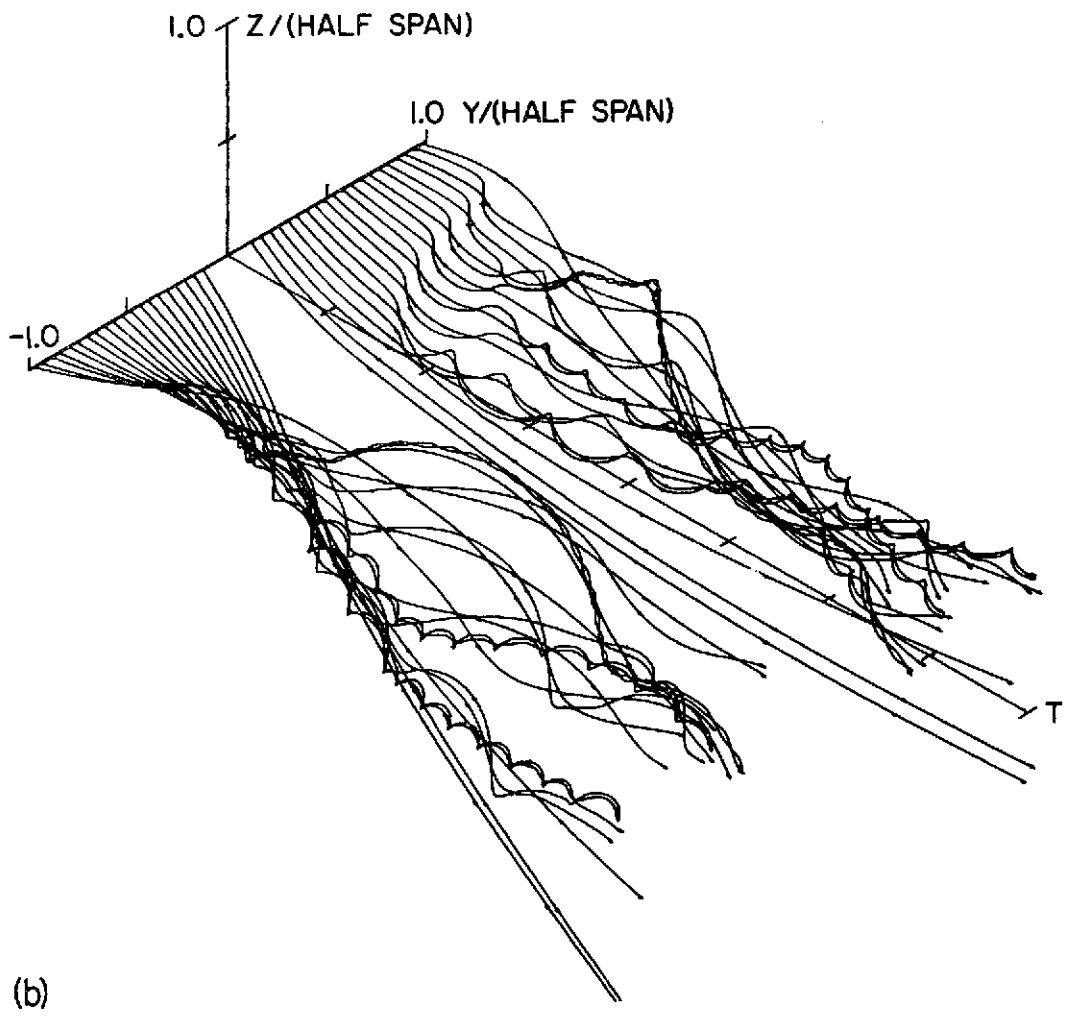
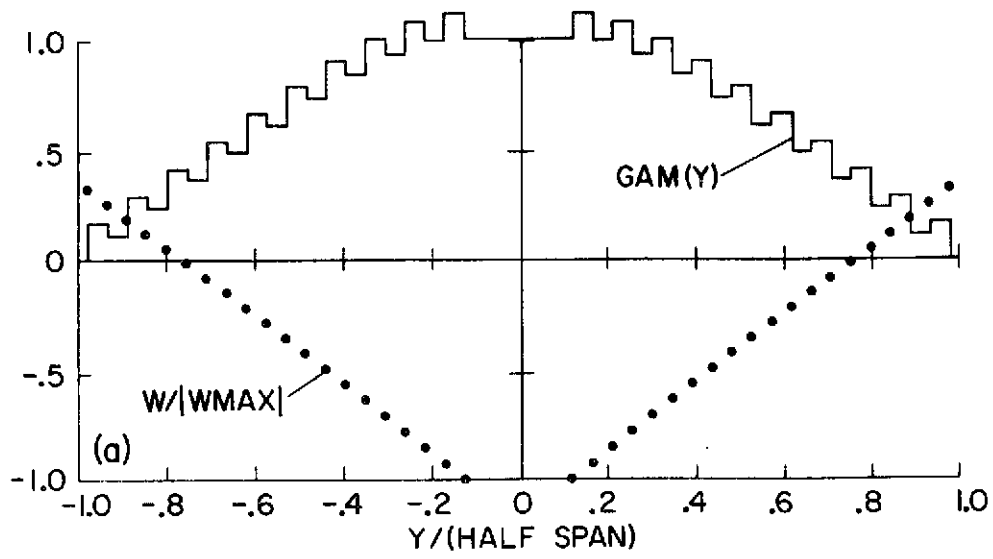
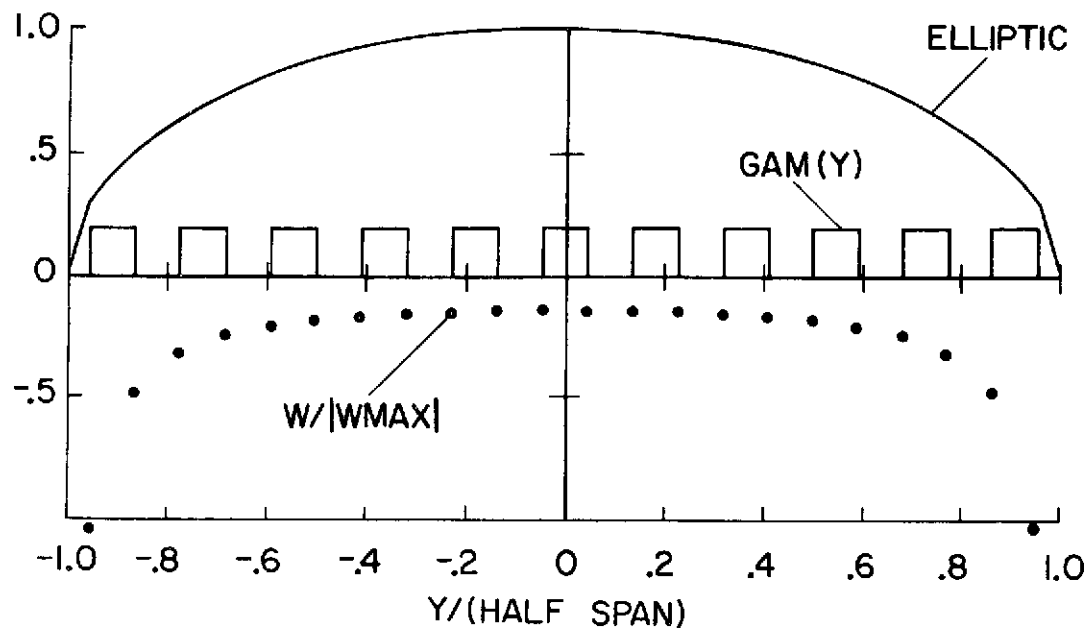
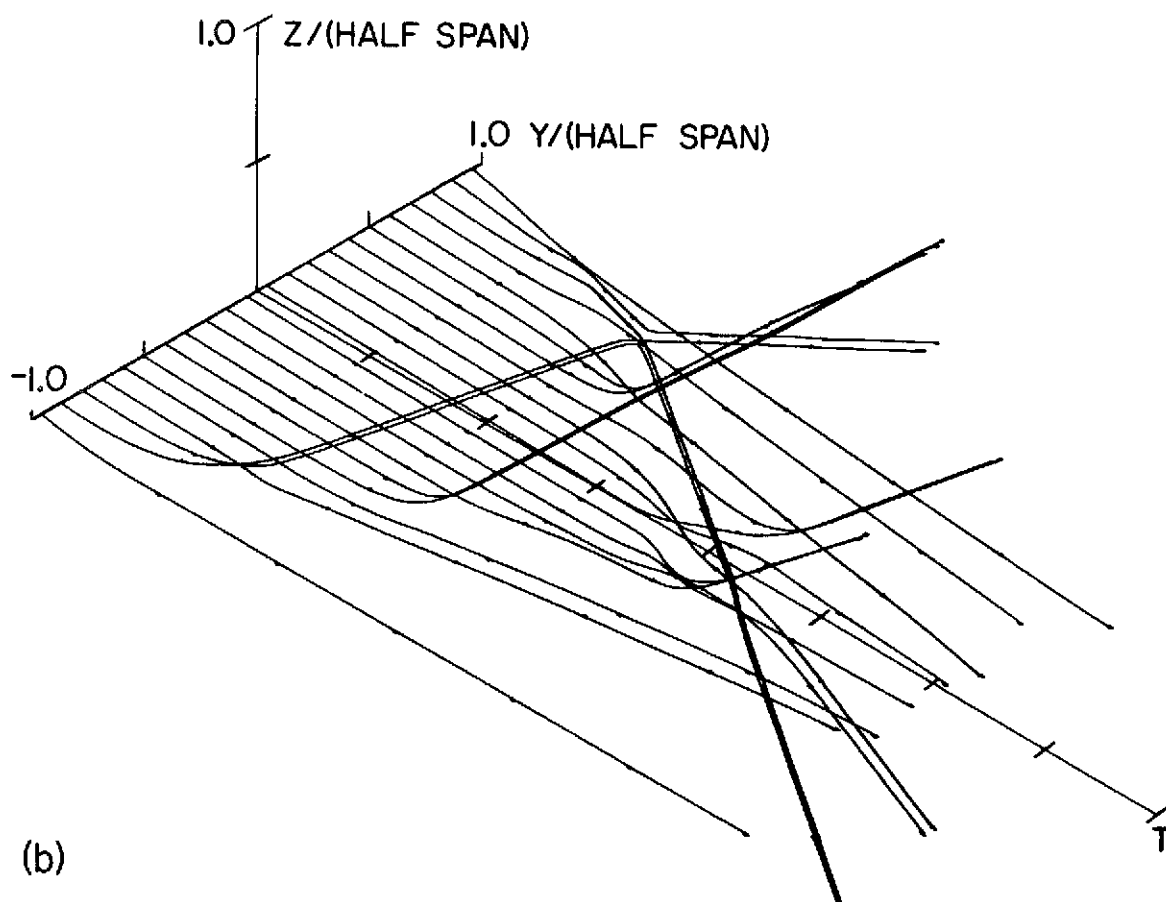


Fig. 13



(a)



(b)

Fig. 14

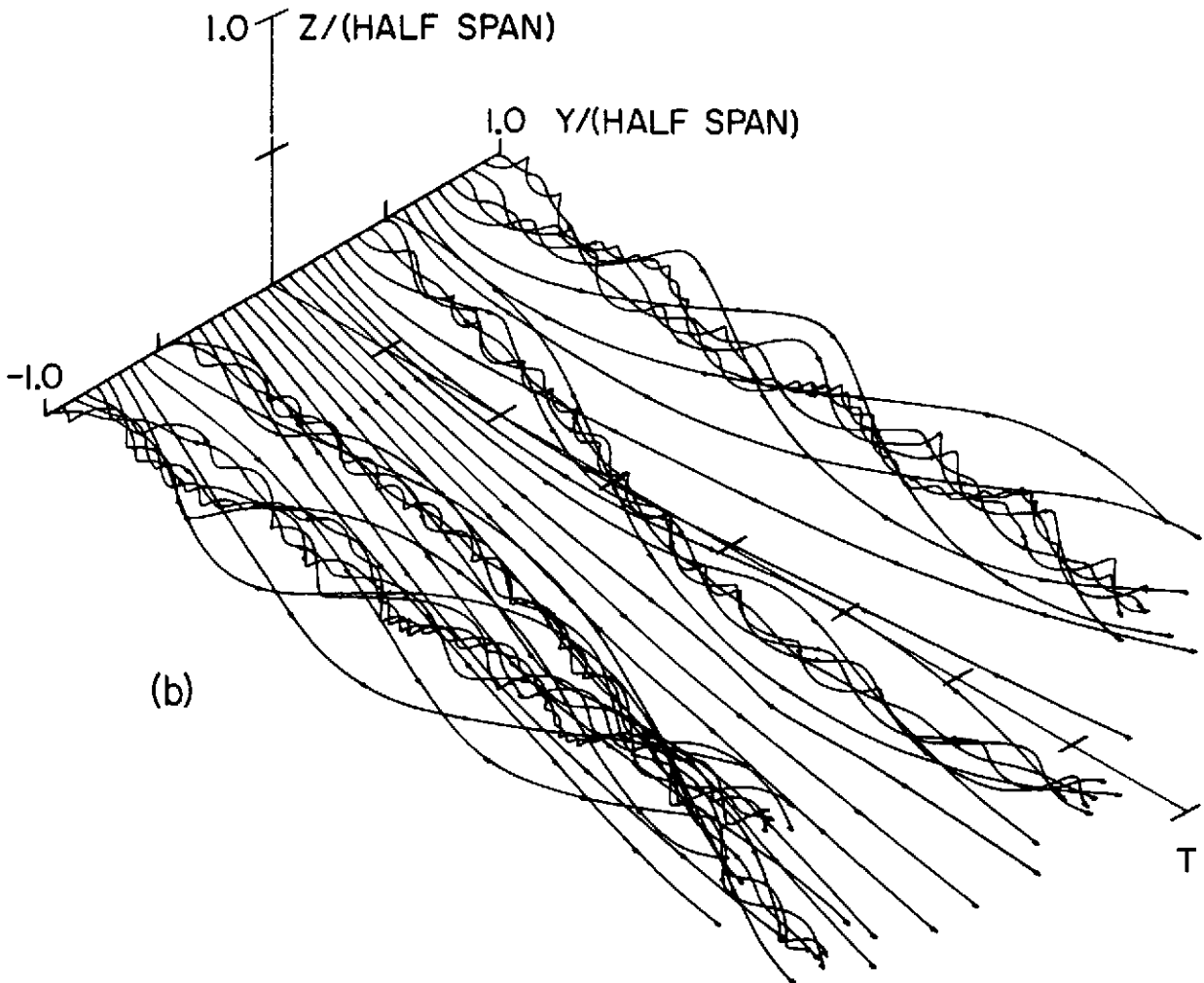
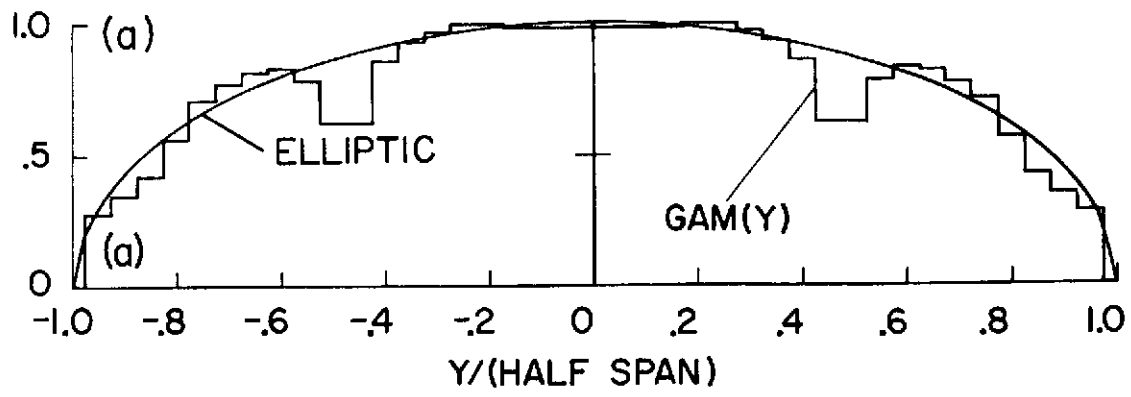


Fig. 15

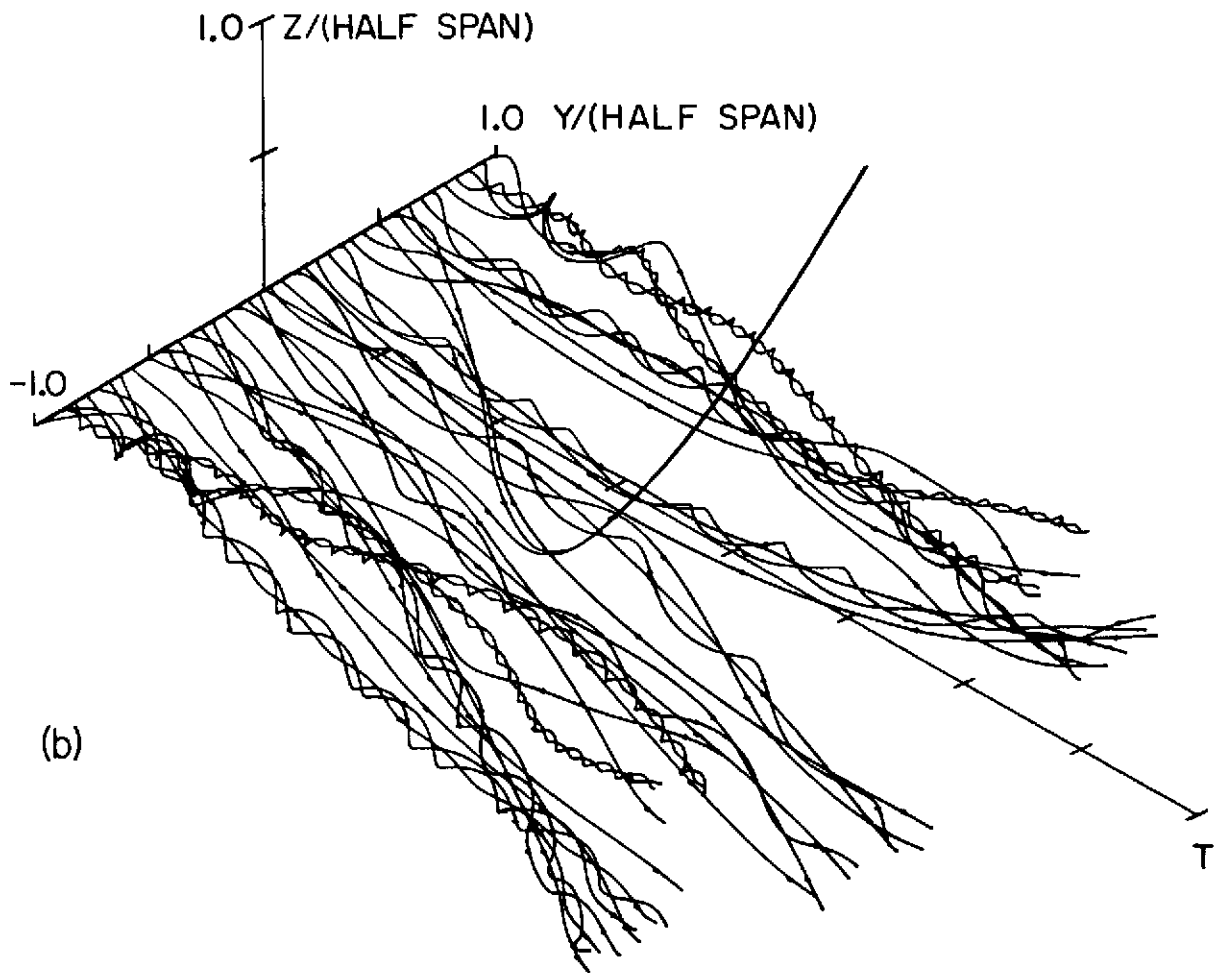
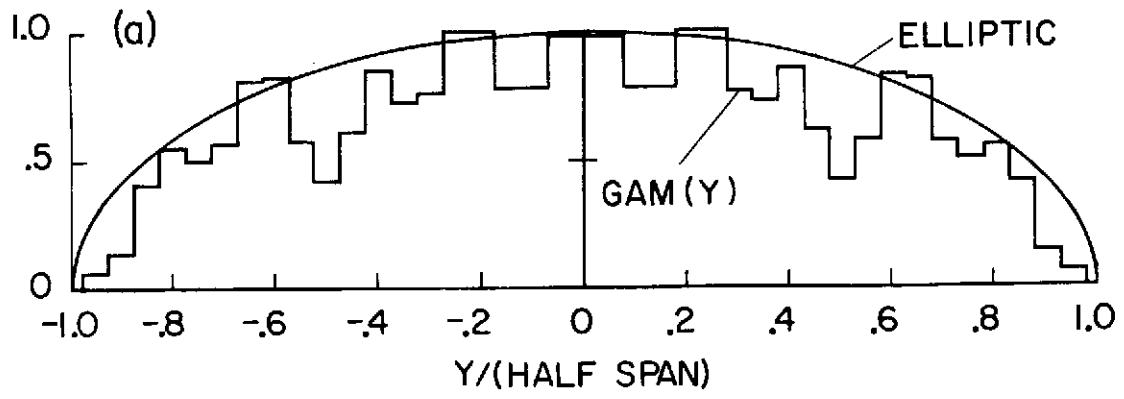


Fig. 16